Analysis of Traveling Performance for Orchard Weeding Robot based on GNSS

Jintack Jeon[1,2], Hoseung Jang[1], Changju Yang[1], Kyoung-do Kwon[1], Youngki Hong[1], Gookhwan Kim[1*]
Department of Agricultural Engineering, National Institute of Agricultural Science, Jeonju, Republic of Korea[1]
Department of Agricultural Machinery Engineering, Chungnam National University, Daejeon, Republic of Korea[2]
jeonjt@korea.kr, hsijjang@korea.kr, nobel1st@korea.kr, kwonkd89@korea.kr, sanm70@korea.kr, meceng93@korea.kr[*]

***Abstract*— Weeding is a necessary work for the growth and quality of crops, and large and small accidents occur or burden the workers during weeding. Therefore, to keep workers safe and reduce work burden, research on weeders is being conducted, and research on unmanned weeders capable of weeding without workers is also being conducted. In this study, we developed and tested a path-following algorithm that can drive along pre-recorded route points for unmanned driving and weeding of weeding robots. The path estimation algorithm used in this study determined the driving direction of the weeding robot based on the geometric model, which defined the steering angle as the angle between the global path and the straight line formed from the center coordinate point of the robot to the target waypoint. As a result of the driving test, the average driving error, maximum driving error, and maximum driving error width compared to the planned route were 0.1048m, 0.2341m, and 0.434m in the straight driving section, and 0.1279m, 0.4101m, and 0.5208m in the turning section.**

Keywords—weeding robot, path-following, Track Vehicle, Orchard, RTK-GNSS

I. Introduction

Weeding is one of the essential tasks for the growth and quality of crops among various tasks performed in agricultural fields [(1)]. However, weeding is a heavy burden on workers, and accidents frequently occur. As a related example, in the case of a lawn mower, the blade is broken or foreign substances such as stones are splashed on the worker[(2)]. In addition, in the case of weeding using a tractor-mounted mower or riding mower, there is a burden on the worker to drive and operate the work machine due to the aging and femaleization of agriculture.

Research on weeders to keep workers safe and reduce work burden has been conducted so far, and as a preceding study, research on weeding robots that autonomous driving using induction cables or remote control driving is being conducted. The guided autonomous driving system with induction cables has the advantage of continuing to be used once buried, but the cost of burial in a large space such as an orchard can be an economic burden for workers, and it can be easily disconnected when digging with work tools such as shovels and hoes[(3)]. In the remote control system that uses remote signals to control driving and implementation, the operator must be within a certain range for the signal connection between the controller and the robot, which is also a burden on the operator[(4)].

In this study, we developed and tested a path-following algorithm that enables driving along pre-recorded waypoints using RTK-GNSS. The purpose of this study is to develop an algorithm for path-following driving using RTK-GNSS and to check whether it can be applied in the field to reduce the burden on workers in the process of directly or indirectly operating the machine.

II. Kinematics Robot Model

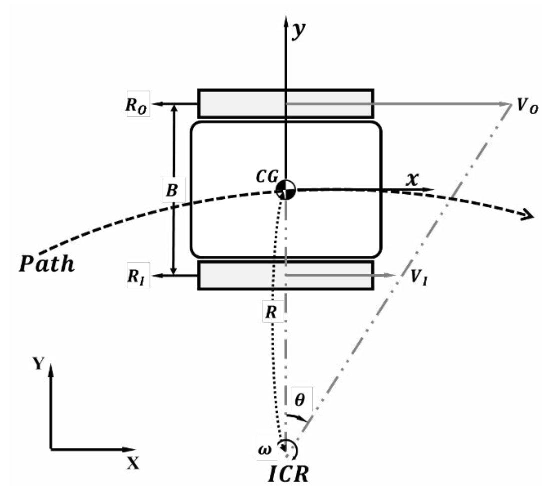

Fig. 1. Kinematics model of the weeding robot

The unmanned weeding robot used in this study is a two-dimensional model, and it is assumed that it only moves in a plane on the ground. In Figure 1, the center of gravity(CG) of the weeding robot is expressed as a kinematic equation as shown in a fixed coordinate(X, Y). In addition, assuming that the weeding robot moves in the x-axis direction and rotates to the right. The inner and outer orbit tracks are marked with 'I' and 'O' in the lower subscripts based on the Instantaneous Center of Rotation(ICR). ICR is located on the straight line formed by both track axes and is determined by the ratio of the rotational speeds of both tracks[(5,6)].

In an orbit track wheel type weeding robot determines the direction of driving and speed based on the input of the linear velocity and angular velocity. v is the center linear velocity value of both tracks(V_O, V_I), and w is the angular velocity value of the driving robot. From the relationship between linear and angular velocity, the angular velocities of the outer and inner tracks are defined as w_O , w_I respectively. Assuming no slip, the contact point velocity between each track and the ground is described as Equation (1). In this case, r represents the track wheel radius.

$$V_O = rw_O; \quad V_I = rw_I \tag{1}$$

The linear velocity and the angular velocity of the robot can be expressed by Equations (2) and (3), and have a relationship of Equation (4). In this case, B represents the interval between both tracks.

$$v = \frac{V_O + V_I}{2} = \frac{r(w_O + w_I)}{2} \quad (2)$$

$$w = \frac{V_O - V_I}{B} = \frac{r(w_O - w_I)}{B} \quad (3)$$

$$\begin{bmatrix} v \\ w \end{bmatrix} = \begin{bmatrix} \frac{r}{2} & \frac{r}{2} \\ \frac{r}{B} & \frac{r}{B} \end{bmatrix} \begin{bmatrix} w_O \\ w_I \end{bmatrix} \quad (4)$$

Differentiation of the robot coordinates (x, y) and steering angle(θ) over time is expressed as Equation (5), which represents the relationship between the instantaneous change$\left(\dot{x}\ \dot{y}\ \dot{\theta}\right)^t$ in robot coordinates and the robot's linear velocity and angular velocity$(v\ w)^t$. Through this, it will be confirmed that the posture and position of the robot are determined by the speed ratio of both tracks.

$$\begin{pmatrix} \dot{x} \\ \dot{y} \\ \dot{\theta} \end{pmatrix} = \begin{pmatrix} cos\theta & 0 \\ sin\theta & 0 \\ 0 & 1 \end{pmatrix} \begin{pmatrix} v \\ w \end{pmatrix} \quad (5)$$

The velocities V_O and V_I of both tracks are proportional to the distances R_O and R_I from the ICR to each track and are expressed as Equation (6). according to the relation above equation, R_O and R_I have the relationship shown in Equation (7), and the turning radius of the orbit track is expressed by Equation (8).

$$V_O : R_O = V_I : R_I \quad (6)$$

$$R_O = R + \frac{B}{2}; \quad R_I = R - \frac{B}{2} \quad (7)$$

$$R = \frac{B(V_I + V_O)}{2(V_O - V_I)} \quad (8)$$

III. Path Following Algorithms and Controllers

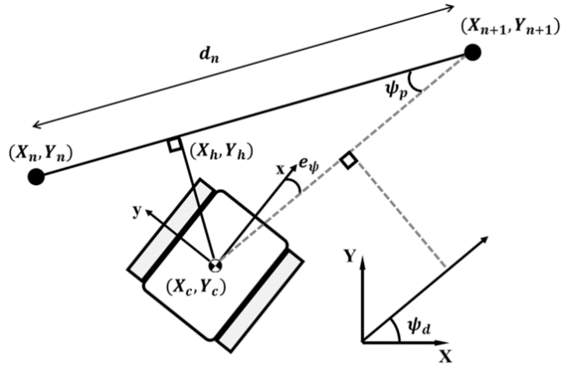

Fig. 2. Concept of the path-tracking algorithm

The path-following algorithm applied in this study is a path-following method based on a kinematics model using the target waypoint(X_{n+1}, Y_{n+1}), and the central coordinate point of robot(X_C, Y_C). Using the kinematics model shown in Figure 2, the steering angle of the weeding robot is calculated and the driving direction is determined. The angle of the path vector in global coordinates to determine the driving direction angle is calculated as in Equation (9). To calculate the direction angle of the robot, the angle between the global path and the straight line formed from the center coordinate point of the robot to the target waypoint is defined as robot direction angle(ψ_p), which is calculated by Equation (10). The error between the robot direction and the driving direction angle is defined by Equation (11), and a PID controller is established by Equation (12) for a control command converging the defined error to zero.

$$\psi_d = \tan^{-1}\left(\frac{Y_{n+1} - Y_n}{X_{n+1} - X_n}\right) \quad (9)$$

$$\psi_p = \tan^{-1}\left(\frac{Y_{n+1} - Y_c}{X_{n+1} - X_c}\right) \quad (10)$$

$$e_\psi = \psi_d - \psi_p \quad (11)$$

$$k_P e_\psi + k_I \dot{e_\psi} + k_D \ddot{e}_\psi = 0 \quad (12)$$

IV. Path Generation and Driving Test

The model of the weeding robot used for the driving test is shown in Figure 3. The specification of the robot is expressed in Table 1 below. RTK-GNSS module (TDR-3000, SYNEREX, Korea) was installed in this weeding robot. Route point generation and path following tests were performed at the driving test field in the Department of Agricultural Engineering of the Rural Development Administration.

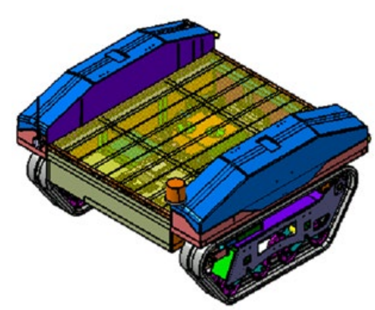

Fig. 3. 3D model of Unmanned Weeding robot platform

TABLE I. Specification of Weeding Robot Platform

Description	Specification
Size	930 x 1,400 x 1,520 mm
DrivingSpeed	Max. 4 Km/h
Drive Source	Electric Battery 50.8V/120Ah*2ea (12.2kWh)

The path planning was set to a total travel distance of 42.9m, traveling back and forth in a U-shape to an arbitrary point using the signal of the RTK-GNSS module. It was set to straight drive 18.31m along the orchard row from the starting point, turn 6.28.m away from the end of the road in the orchard, move to the next orchard row, and straight drive 18.31m.

The driving test was repeated three times on an asphalt pavement without a slope. The driving linear speed was fixed at 2 km/h, and when it deviated from the route, the speed of each wheel was changed to converge to the planned route within the error range. For the driving error, the result of calculating the vector dot product Equation (13) for the shortest distance from the planned path to the robot coordinates was used.

$$Lateral\ Error = \frac{(X_n - X_C)(Y_{n+1} - Y_C) - (Y_n - Y_C)(X_{n+1} - X_C)}{\sqrt{(X_{n+1} - X_C)^2 + (Y_{n+1} - Y_C)^2}} \quad (13)$$

Figure 4. shows the result of the lateral error according to the driving distance of the 1st driving test conducted on the planned route. In the straight section, it was driven within the maximum deviation of 20 cm from the planned route, and it was confirmed that it converged even if it deviated from the driving route. In the turning section, the maximum deviation value within 30 cm was confirmed.

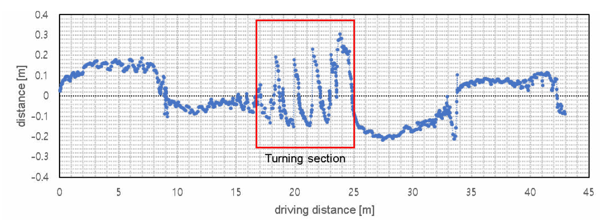

Fig. 4. Lateral position error according to driving distance

Figure 5. shows the total driving test results, with the maximum average driving error (blue), maximum driving error(green), and maximum driving error width(red) compared to the planned route. 0.1048m, 0.2341m, 0.434m in the straight driving section, and 0.1279m, 0.4101m, 0.5208m in the turning section.

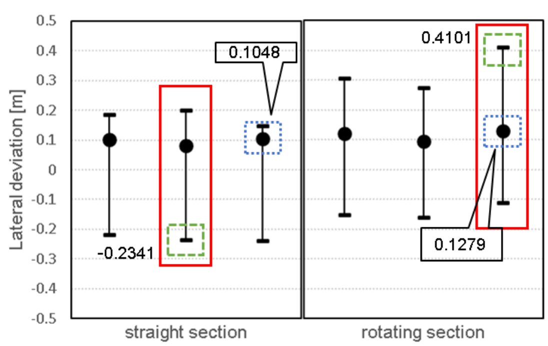

Fig. 5. Lateral deviation according to driving section

Considering that the width between rows of fruit trees in the current apple orchard is 3~4m, this weeding robot is expected to be available for orchard field testing. Advanced technology development in orchards is expected to sustain sustainable agricultural production even in the aging and labor-short farms in orchard weeding.

Acknowledgment

This study was supported in part by the Rural Development Administration grants (No.PJ015595012023, Research on Intelligent weeding robot for apple orchard)

References

[1] I.Y. Lee, J.E. Park, T.S. Park, S.T. Lim, and B.C. Moon, “Fact-finding survey on paddy, upland and orchard herbicides use at farmer’s level,” Korean Society of Weed Science, vol.21(1), pp.58-64, 2001.

[2] I.G. Kang, C.S. Park, H.S. Ryu, S.J. Heo, Y.S. Chae, and W.J. Jeong, “Clinical analysis of Ocular Trauma Induced by Lawn Trimmers,” The Korean Society of Traumatology, vol. 24(2), pp.61-67, 2011.

[3] H.S. Jang and I.J. Jang, “Development of the weeding robot for base part of trees in orchard,” Journal of Agricultural Machinery Engineering, vol. 24(1), pp.454-454, 2019.

[4] C.H. Park “Development of steering clutch and remote controller for small mower,” MS thesis, Daegu, Rep. Korea: Department of Bio-industrial Machinery Engineering, Kyungpook National University, 2013.

[5] J.H. Sohn, C.H. Lee, Y.J. Kim, and S.S. Kim, “Evaluation of Path Tracking Performance of a Self-driving Tracked Vehicle,” Transactions of the Korean Society of Mechanical Engineers, vol.66(3), pp.1167-1176, 2022.

[6] K.T. Kim, M.C. Kang, J.H. Lee, J.W. Ha, and G.W. Park, “A Study on the Controllability of Clutch/Brake Steering for Low-Speed Tracked Vehicles,” Journal of Power System Engineering, vol. 25(5), pp.51-60, 2021.